Diagn Interv Radiol 2011; 17:216–222

CHEST IMAGING

ORIGINAL ARTICLE

Chest radiography and CT findings in patients with the 2009 pandemic (H1N1) influenza

Elif Karadeli, Zafer Koç, Şerife Ulusan, Gürcan Erbay, Yusuf Ziya Demiroğlu, Nazan Şen

PURPOSE

To present chest radiography and thoracic computed tomography (CT) findings for patients with pandemic influenza A (H1N1) from November–December 2009 and to explore any differences compared to previously reported imaging findings.

MATERIALS AND METHODS

Fifty-two hospitalized patients with pandemic influenza (H1N1) were included in the study. All of the patients underwent chest radiography, and 28 patients were also evaluated by thoracic CT. Group 1 comprised 24 (46%) patients with no identified risk factors for H1N1 influenza infection. Group 2 comprised the remaining 28 (54%) patients with identified risk factors. The distribution of lung involvement, consolidation, ground-glass opacity (GGO), lymph nodes, and pleural effusion were evaluated.

RESULTS

Abnormal findings were observed in 85% of the patients. Bilateral lung involvement was present in 80% of the patients. The most common finding was a mixture of GGO and air-space consolidation. Lower zone predominance occurred in 89% of group 1 and 85% of group 2 patients. The involvement was observed most frequently in the peripheral and central perihilar areas of the lung in 80% of the patients. The extent of disease was greater in group 2 patients with the involvement of three or more lung zones in 62% of the patients.

CONCLUSION

The most common imaging finding for lung involvement was a mixture of air-space consolidation and GGO with a patchy pattern and lower/middle zone predominance. Pulmonary involvement of the disease was more extensive than that described in previous reports.

Key words: • *thorax* • *computed tomography* • *influenza A virus, H1N1 subtype* • *pneumonia, viral*

From the Departments of Radiology (E.K. ✉ *elifkaradeli@gmail.com*, Z.K., Ş.U., G.E.), Infectious Diseases and Clinical Microbiology (Y.Z.D.), and Chest Diseases (N.Ş.), Başkent University Faculty of Medicine, Adana Teaching and Medical Research Center, Adana, Turkey.

Received 2 February 2010; revision requested 24 June 2010; revision received 1 July 2010; accepted 6 July 2010.

Published online 12 August 2010
DOI 10.4261/1305-3825.DIR.3337-10.1

The 2009 pandemic (H1N1) influenza affected a large group of patients across the world, especially due to the early arrival of the winter influenza season in the Northern Hemisphere. More than 206 countries and overseas territories or communities reported laboratory-confirmed cases of H1N1 in 2009, including over 6,770 deaths (1), and more people are expected to be affected by this disease in the near future. The first cases of novel influenza A (H1N1) infection were observed in Southern California counties in April 2009 and then spread worldwide (2). On June 11, 2009, the World Health Organization declared a phase 6 influenza pandemic (3, 4). The influenza A (H1N1) virus is a subtype of the influenza A virus, which is the most common cause of influenza in humans in 2009. Unfortunately, the most virulent influenza viruses are type A, and they mutate easily and quickly (5, 6).

The symptoms of H1N1 infection may be similar to seasonal influenza, and hospitalization is not usually required. The virus can infect the lower respiratory tract and cause rapidly progressive pneumonia, especially in children and younger adults (7). Some chest radiography and chest computed tomography (CT) findings have been reported for H1N1 infection during the early phase (May–June 2009) of the spread of disease (8–10). The aim of the present study was to explore the chest radiography and thoracic CT findings of patients with confirmed pandemic influenza A (H1N1) infection in November and December of 2009 and to explore any differences compared to previously reported CT findings.

Materials and methods

This study was approved by our institutional review board, and written informed consent was obtained from each subject. Between November 1 and December 18, 2009, 52 hospitalized patients (31 women and 21 men) with a confirmed diagnosis in our hospital of pandemic 2009 influenza A (H1N1) were included in the study. The age of the patients ranged from 18 to 70 years (mean±SD, 41±1.3 years). The patients were divided into two groups. Group 1 comprised 24 (46%) patients with no identified risk factors for H1N1 influenza infection. Group 2 comprised the remaining 28 patients (54%) with the following identified risk factors: heart disease (n=3), chronic obstructive lung disease (n=4), pregnancy (n=4), lymphoma (n=2), end-stage renal disease (n=2), diabetes mellitus (n=4), sickle cell anemia (n=2), morbid obesity (n=4), or systemic lupus erythematosus (n=3). Some of these patients were current smokers. The patients in group 2 had a higher mean age than did those in group 1 (43.9 years vs. 37.2 years).

All of the patients had flu-like symptoms. Oropharyngeal and/or nasopharyngeal specimens of all patients were evaluated by real-time polymerase chain reaction (PCR) and were positive for pandemic novel influenza A (H1N1).

All of the patients underwent chest radiography, and 28 patients were also evaluated by thoracic CT at our hospital. CT examinations were performed using a 4-MDCT scanner (Somatom Sensation 4, Siemens Medical Solutions, Erlangen, Germany). A routine thoracic CT protocol was employed for 18 patients. Seventeen patients underwent high-resolution CT (HRCT), including 7 patients who received both HRCT and thoracic CT. Routine thoracic CTs were obtained during the arterial phase after administering a 120 to 150 mL IV bolus of 300 mg/mL nonionic contrast material (Optiray, Covidien, Pointe Claire, Quebec, Canada) at a rate of 3–5 mL/s. The thoracic CT parameters were as follows: 90 mAs, 120 kVp; scan time, 26 s; slice thickness, 5 mm; contiguous 1-mm collimation; table speed, 12 mm/s; gantry rotation, 360° per 0.5-s with a resultant pitch value of 1.5. Our HRCT protocols were as follows: 270 mAs and 120 kVp, 1-mm collimations, 1-mm slice thickness, and 10-mm reconstruction intervals.

Two experienced radiologists reviewed all of the chest radiography and CT examinations by consensus. The chest radiography and CT findings were classified as normal or abnormal. The distributions of lung involvement were assessed as unilateral or bilateral and as central perihilar, peripheral, or diffuse (both central perihilar and peripheral). Each lung was divided into upper, middle, and lower zones. The extent of involvement for each zone was evaluated as <20% or >20%; in addition, involvement of 3 or more lung zones was recorded.

The abnormal findings were air-space consolidation (opacification obscuring the underlying vessels), ground-glass opacity (GGO; increased attenuation without obscuring the underlying vessels), nodules, and reticulation. Additionally, lymph node enlargement and pleural effusion, pulmonary embolism, and the presence of an endotracheal tube were also noted.

Results

The patient imaging findings are summarized in Table. Normal radiological findings were observed in only 8 of the 52 (15%) patients; 44 of the 52 (85%) patients presented abnormal findings. Bilateral lung involvement was observed in 35 of the 44 (80%) patients, and the remaining 9 (20%) patients had unilateral lung involvement.

In all of the cases, the most common finding was a mixture of GGO and air-space consolidation; this mixture was seen in 10 of the 18 (56%) group 1 patients and in 18 of the 26 (69%) group 2 patients. Lung abnormalities were most commonly detected in the middle and lower zones. Lower zone predominance occurred in 89% of group 1 and 85% of group 2 patients (Fig. 1).

In group 1, 7 of the 18 (38 %) patients had air-space consolidation only, and 1 of the 18 (6%) had GGO only. The predominant pulmonary imaging finding in group 1 was a patchy air-space consolidation pattern and/or GGO in 11 of the 18 (61%) patients. The other finding was a diffuse consolidation pattern and/or GGO in 7 of the 18 (39%) patients (Figs. 2 and 3).

The predominant pulmonary imaging finding in group 2 was a patchy air-space consolidation pattern and/or GGO in 20 of the 26 (77%) patients. The other finding was a diffuse air-space consolidation pattern and/or GGO in 6 of the 26 (23%) patients.

Involvement was more common in the peripheral and central perihilar areas of the lung in 35 of the 44 (80%) patients. The most common localization in both groups was diffuse, which was observed in 12 of the 18 (67%) patients in group 1 and 23 of the 26 (88%) patients in group 2. Three or more lung zones were involved in 25 of the 44 (57%) patients. The extent of disease was greater in group 2 patients, in which the involvement of three or more lung zones was observed in 16 of the 26 (62%) patients. Minimal pleural effusion was detected on the CT in 5 (11%) patients (Figs. 4 and 5). Milimetric (short axis diameter, <10 mm) lymph nodes in the mediastinum and hilar regions were observed on the CT in 13 of the 44 (30%) patients. In

Table. Radiographic and CT findings in 52 hospitalized patients with a confirmed diagnosis of H1N1 influenza

	Group 1[a] n=24 (46%)	Group 2[b] n=28 (54%)	All n=52 (100%)
Normal radiologic findings	6 (25%)	2 (7%)	8 (15%)
Abnormal radiologic findings	18 (75%)	26 (93%)	44 (85%)
Extent of lung involvement			
a. <20%	6/18 (33%)	4/26 (15%)	10/44 (23%)
b. >20%	3/18 (17%)	6/26 (23%)	9/44 (20%)
c. Three or more involved zones	9/18 (50%)	16/26 (62%)	25/44(57%)
Patterns of abnormality[c]			
a. Consolidation only	7/18 (38%)	8/26 (31%)	15/44 (34%)
b. Ground-glass opacity only	1/18 (6%)	0	1/44 (2%)
c. GGO+ consolidation	10/18 (56%)	18/26 (69%)	28/44 (64%)
1. Patchy pattern	11/18 (61%)	20/26 (77%)	31/44 (70%)
2. Diffuse pattern	7/18 (39%)	6/26 (23%)	13/44 (30%)
Distributions of abnormality[c]			
a. Lower zone predominance	16/18 (89%)	22/26 (85%)	38/44 (86%)
b. Middle zone predominance	2/18 (11%)	4/26 (15%)	6/44 (14%)
1. Central perihilar	0	1/26 (4%)	1/44 (2%)
2. Peripheral	6/18 (33%)	2/26(8%)	8/44 (18%)
3. Diffuse	12/18 (67%)	23/26 (88%)	35/44 (80%)
Final outcome, death	1/24 (4%)	7/28 (25%)	8 /52 (15%)

[a]Group 1, patients without identified risk factors for H1N1 influenza infection
[b]Group 2, patients with a risk factor for H1N1 influenza infection
[c]According to CT (n=28) and radiographic (n=24) findings

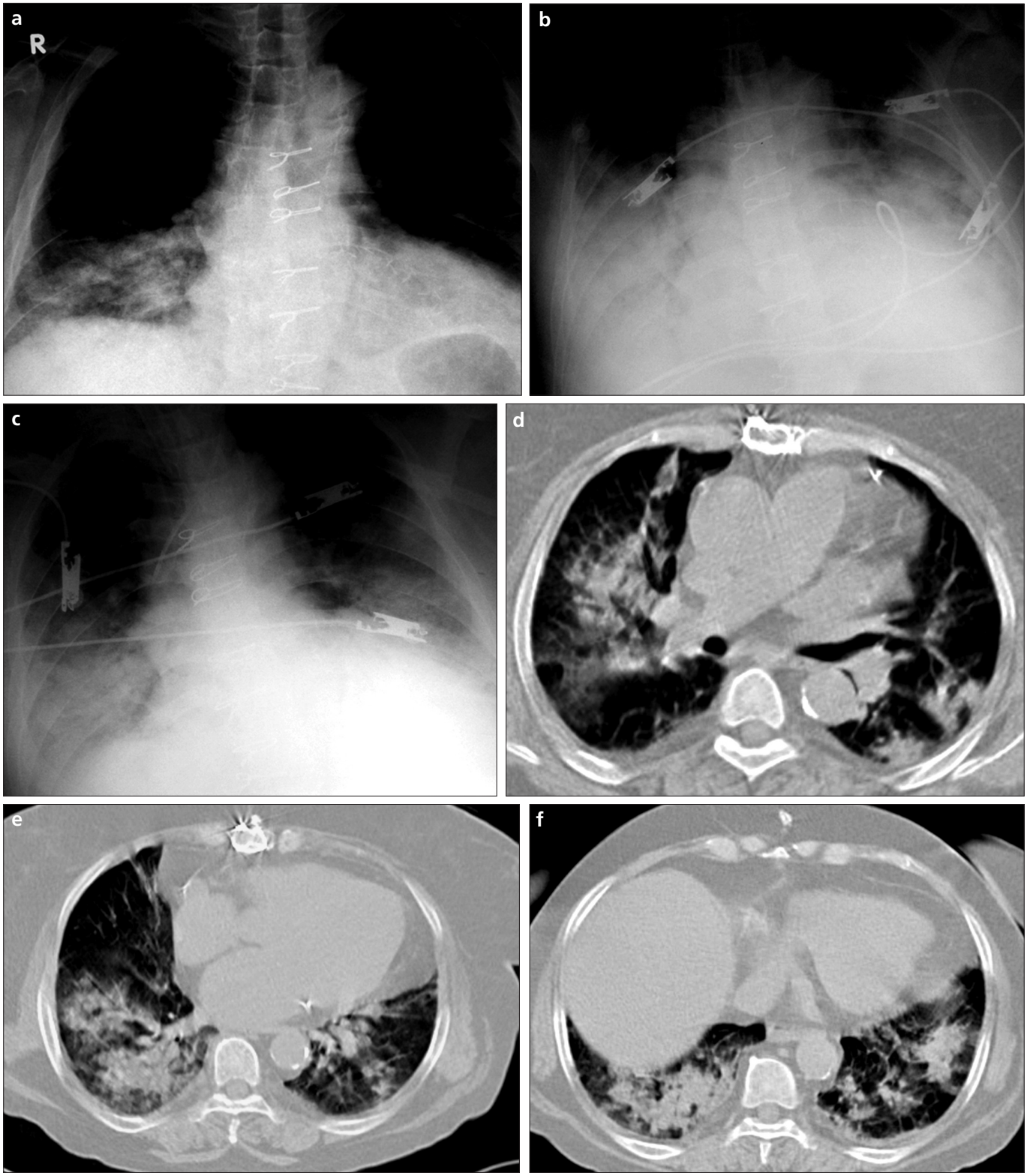

Figure 1. a–f. A 52-year-old woman with systemic lupus erythematosus, diabetes mellitus, and laboratory-confirmed influenza A (H1N1) who died. Initial chest radiograph **(a)** showing consolidation only in the right basal segment. Chest radiograph **(b)** obtained after 1 day revealing progression, and consolidation apparent in both lower lung zones. Follow-up chest radiograph **(c)** on the third day showing a continuous progression of the lung findings. Axial CT images **(d–f)** showing air-space consolidation with a patchy pattern and ground-glass opacities in the peripheral and central perihilar areas of both lung zones.

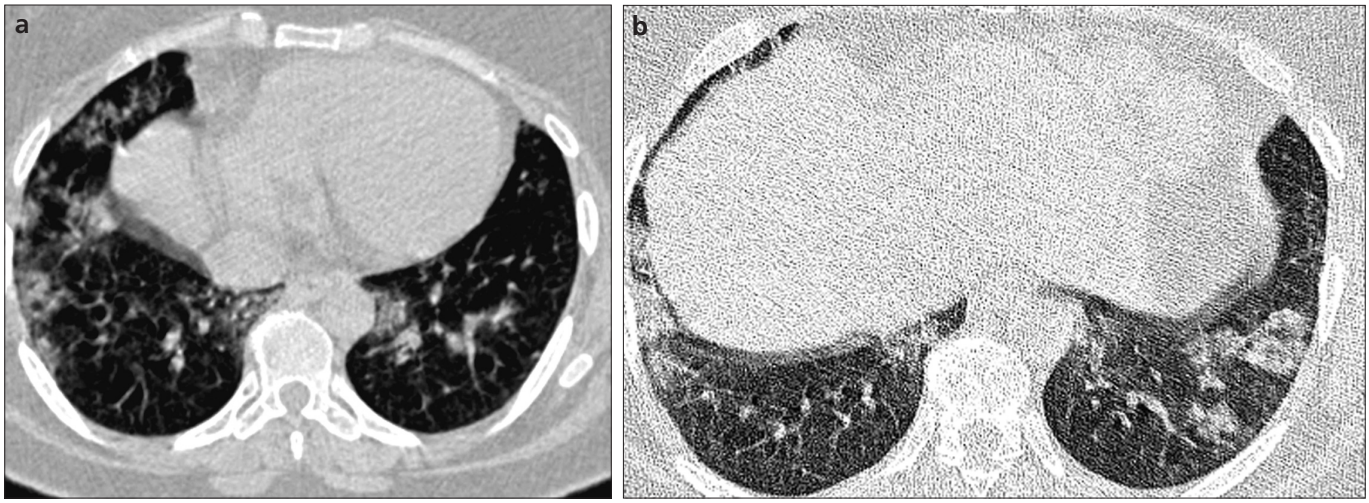

Figure 2. a, b. A 37-year-old woman diagnosed with influenza A (H1N1). High-resolution CT images **(a, b)** showing air-space consolidation with a patchy pattern in both the lower and middle zones, especially in the peripheral lung areas.

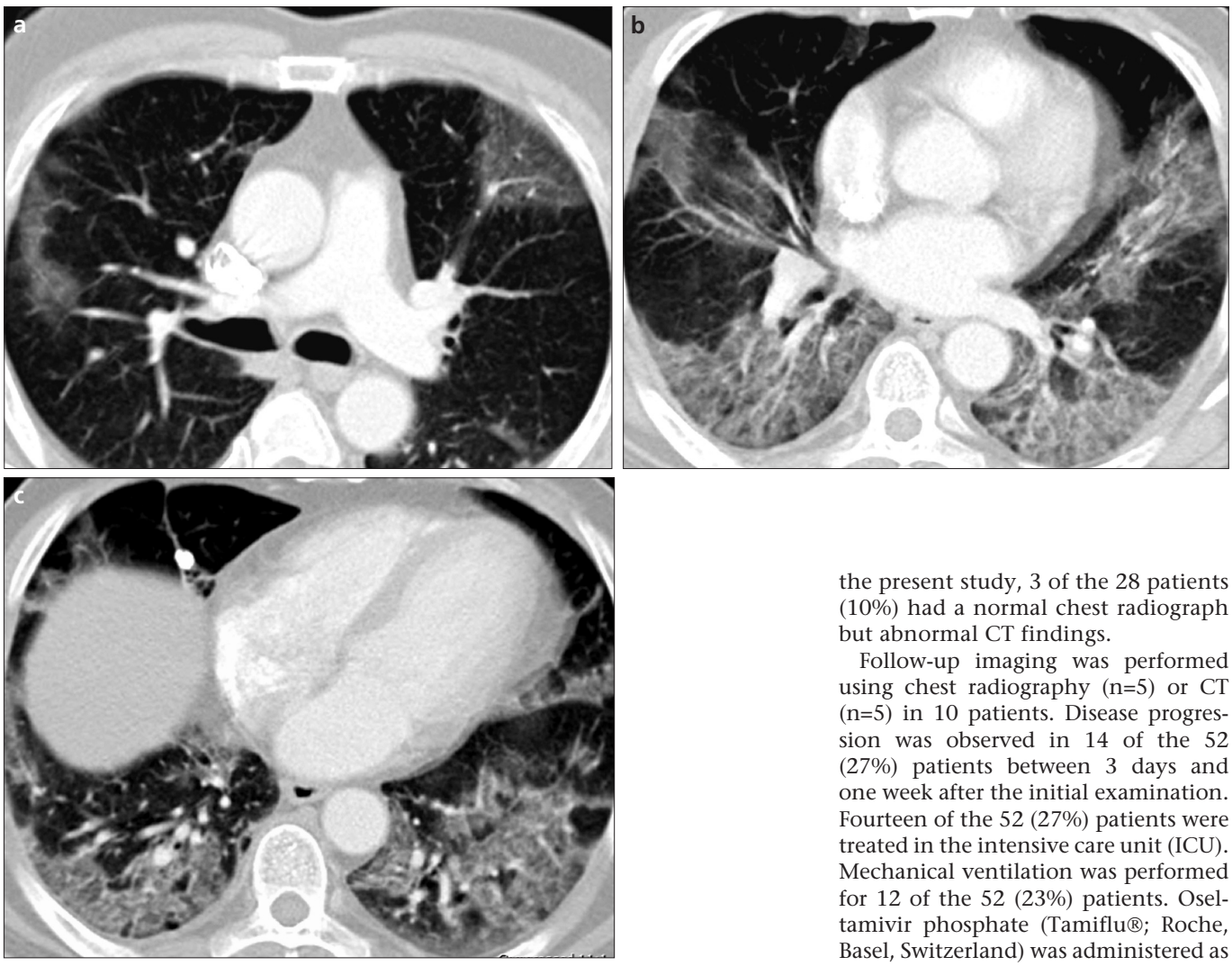

Figure 3. a–c. A 61-year-old man diagnosed with influenza A (H1N1). Axial thorax CT images **(a–c)** showing a patchy pattern of air-space consolidation and involvement of peripheral lung areas with lower and middle zone predominance.

the present study, 3 of the 28 patients (10%) had a normal chest radiograph but abnormal CT findings.

Follow-up imaging was performed using chest radiography (n=5) or CT (n=5) in 10 patients. Disease progression was observed in 14 of the 52 (27%) patients between 3 days and one week after the initial examination. Fourteen of the 52 (27%) patients were treated in the intensive care unit (ICU). Mechanical ventilation was performed for 12 of the 52 (23%) patients. Oseltamivir phosphate (Tamiflu®; Roche, Basel, Switzerland) was administered as an antiviral treatment at a dose of 150 mg twice daily for ICU patients and 75 mg twice daily for the remaining patients. Unfortunately, 8 of the 52 patients (15%) died during the treatment (7 patients in group 2 and 1 patient in

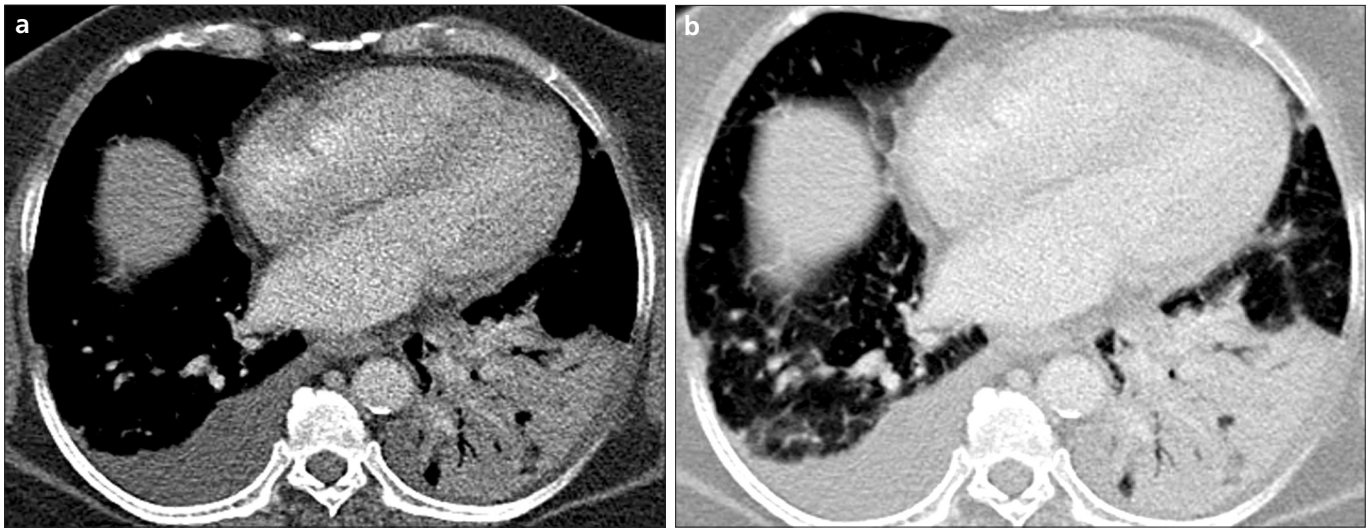

Figure 4. a, b. A 61-year-old woman diagnosed with influenza A (H1N1). Thoracic CT images with mediastinal **(a)** and parenchymal windows **(b)** showing lobar pneumonia in the left lower lobe and pleural effusion in the right lung.

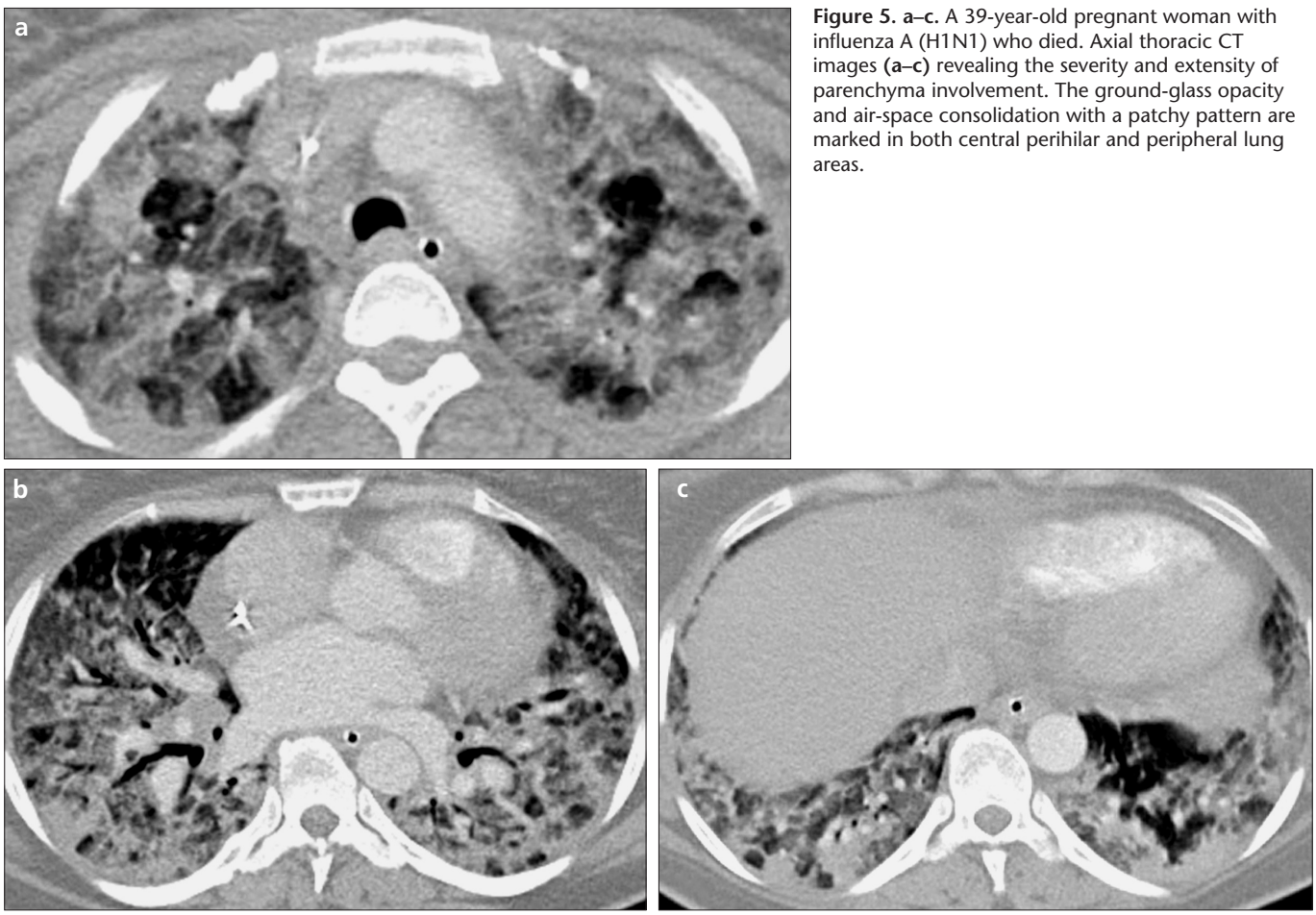

Figure 5. a–c. A 39-year-old pregnant woman with influenza A (H1N1) who died. Axial thoracic CT images **(a–c)** revealing the severity and extensity of parenchyma involvement. The ground-glass opacity and air-space consolidation with a patchy pattern are marked in both central perihilar and peripheral lung areas.

group 1) (Figs. 5 and 6). The length of hospital stay ranged between 3 days and one month.

Discussion

In this study, we showed that the most common pulmonary involvement findings for the pandemic influenza (H1N1) 2009 virus were air-space consolidation with a patchy pattern and GGO. In general, the radiologic abnormalities in our series were located in the bilateral peripheral and central perihilar areas of the lung with lower-middle zone predominance. We found that lung involvement was more extensive in the high-risk group (group 2) than in group 1. In our series, the extent of disease as a percentage of the lung and the mixture of air-space consolidation and GGO were more exces-

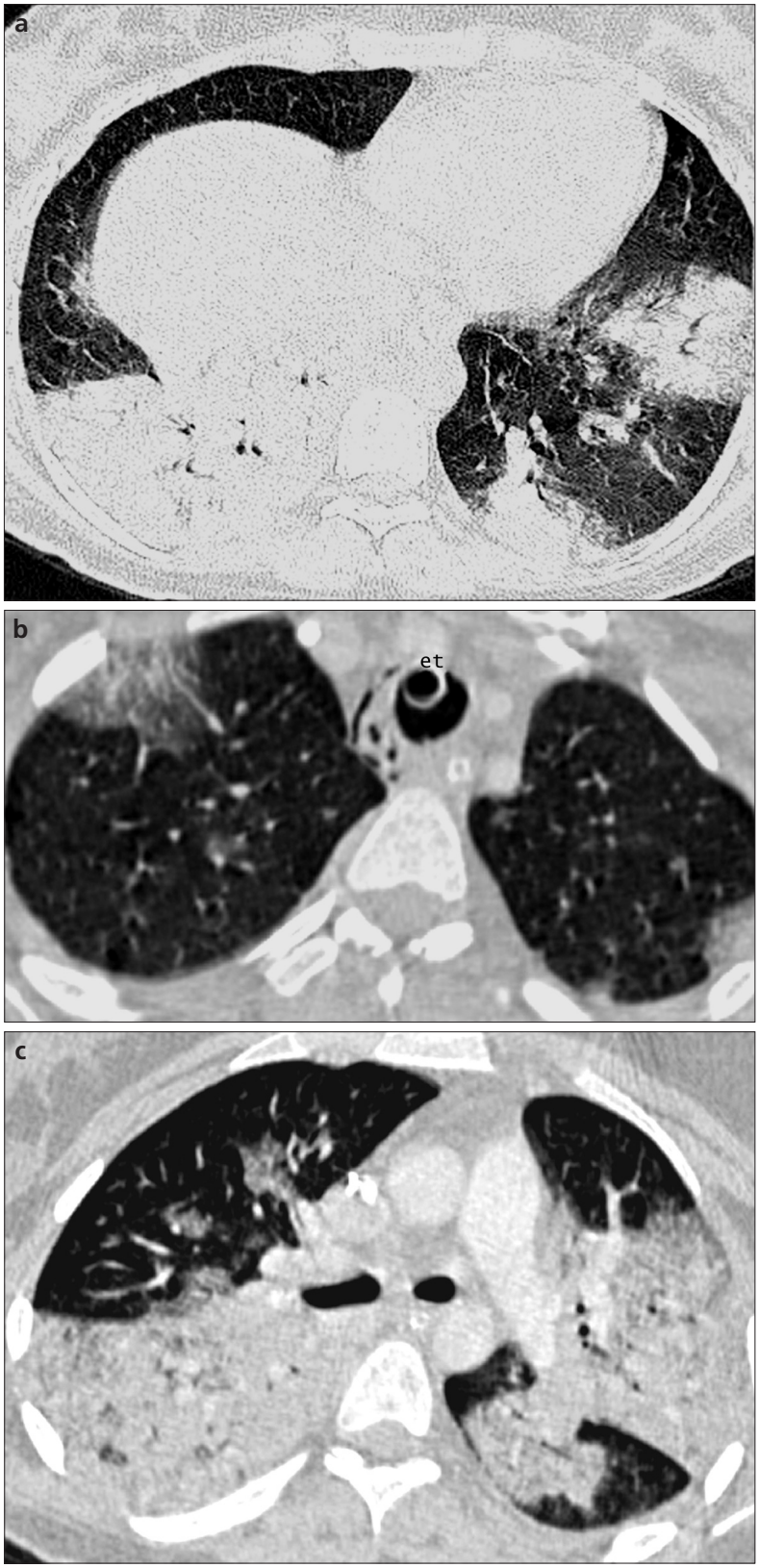

Figure 6. a–c. A 29-year-old pregnant woman with influenza A (H1N1) who died. An axial high-resolution CT image **(a)** showing generalized involvement of the lung parenchyma. On the third day of hospitalization, the patient's condition worsened, and mechanical ventilation was required. During this period, axial thoracic CT images **(b, c)** revealed the increased extent and severity of parenchyma involvement. The lung involvement was diffuse, showing a ground-glass opacity and air-space consolidation with a patchy pattern in both central perihilar and peripheral lung areas (et, endotracheal tube).

sive than those described in previous reports. Nodular involvement or pulmonary embolism was not observed in our series.

The excessive percentage of lung involvement in our series suggests that H1N1 viral pneumonia during the pandemic period was more severe than initially observed and indicates that an investigation of increased virulence or strain changes may be required. The patchy pattern of air-space consolidation was a prominent feature in our series. Although this finding has been reported previously (9), it has not yet been emphasized in a large series (8).

The most common symptoms in patients with influenza A (H1N1) infection are fever, dry cough, sore throat, headache, muscle or joint pain, chills, fatigue, diarrhea, and vomiting, similar to seasonal influenza (7). The symptoms presented in our patients were sore throat, fever, and dyspnea. The pandemic (H1N1) 2009 virus has two distinct features when compared to seasonal influenza. First, it predominately affects children and young adults. Second, an infection of the lower respiratory tract followed by rapidly progressive pneumonia can develop in children and young to middle-aged adults (7). In our study, the mean age of the patients with pandemic influenza (H1N1) was 41 years (age range, 18–70 years), and 65% of the patients were <50 years of age. The patients in group 2 had a higher mean age than did those in group 1 (43.9 vs. 37.2 years).

Pandemic influenza A (H1N1) infection is usually subclinical, occasionally produces respiratory failure, and rarely causes death. Individuals at a higher risk for serious complications include those over 65 years of age and children younger than 5 years. In particular, the underlying medical conditions are very important for disease progression. The worst symptoms and findings appear in conditions such as chronic lung disease (e.g., asthma and chronic obstructive pulmonary disease), conditions associated with immunosuppression (e.g., receiving immunosuppressive medications or HIV positive), chronic cardiac disease (e.g., congenital heart disease and coronary artery disease), diabetes, obesity, pregnancy (especially during the third trimester), and in children with neurodevelopmental conditions (11). In our series, 28 pa-

tients had identified risk factors. The radiologic findings and the extent of lung involvement in group 2 patients were more extensive than were those in group 1 patients. Two of the patients who died during treatment were pregnant, and the infants were delivered by Caesarean section. Five of the patients who died had systemic lupus erythematosus, diabetes mellitus, heart disease, or hypertension. One patient who died had no risk factors or additional diseases.

Primary viral pneumonia is the most common finding in severe cases of influenza and is a frequent cause of death, and secondary bacterial infections occur in approximately 30% of fatal cases. Respiratory failure and refractory shock have been the most common causes of death in patients with H1N1 (12).

Chest radiographic and CT findings in patients with pandemic phase influenza A (H1N1) have not been previously reported. To our knowledge, this is the largest study to present imaging findings for the lung involvement of pandemic H1N1. This is the first study to investigate the pandemic phase of the disease. However, some chest radiography and CT reports are available for patients with novel influenza A (H1N1) infection during the early phase of disease, from April to June 2009 (8–10). Chest radiographic disease findings have been described as abnormalities suggestive of pneumonia, including multilobar and unilobar infiltrates. The radiologic changes in the lung are bilateral patchy alveolar opacities with basal lung predominance or interstitial opacities such as linear, reticular, or nodular shadows (9). GGOs with a patchy pattern and air-space consolidation are the most common thoracic viral pneumonia findings on CT (13).

The distribution of parenchymal abnormalities may be diffuse without zonal predominance, and different zones may be affected. The bilateral lower segment and central area are typically involved, and alveolar disease changes are prominent. Pleural effusion and bilateral multifocal parenchyma involvement may be observed, but pulmonary embolisms have been rarely described (8–10).

Progressive infection has been reported in individuals with H1N1 influenza (8). Similar to previous reports, in the present study, the radiologic changes progressed rapidly within 3 to 7 days in 14 of the 52 (27%) patients. The lung findings first appeared in the lower zones and then rapidly progressed to the middle and upper zones, and the patchy areas progressed to consolidation. Other studies have reported that some patients might require admittance to an ICU and mechanical ventilation to treat a novel influenza A (H1N1) infection (8–10). Mechanical ventilation was required in twelve patients in our study.

Our study had some limitations. First, this study was planned prospectively but was retrospective in nature. Second, the number of patients requiring mechanical ventilation was small; therefore, we did not compare a mechanical ventilation group to a group without mechanical ventilation. This is the first study to describe thoracic CT findings in patients during the pandemic phase of novel influenza A (H1N1) and comprises one of the largest patient groups on this subject in the literature to date. In the near feature, a multicenter study comprising a larger group of patients could explore more detailed imaging findings and determine any changes in disease virulence.

In conclusion, the most common lung imaging finding in pandemic H1N1 was a mixture of air-space consolidation and GGO with a patchy pattern and lower-middle zone predominance. The pulmonary involvement of the disease was more extensive than that described in previous reports.

References

1. World Health Organization. 20 November 2009 Pandemic (H1N1) 2009-update 75.
2. Centers for Disease Control and Prevention (US). Swine influenza (H1N1) infection in two children — Southern California, March–April 2009. Morb Mortal Wkly Rep 2009; 58:400–402.
3. Centers for Disease Control and Prevention. 2008–2009 Influenza season week 32 ending August 15,2009, www.cdcgov/flu/weekly. Accessed September 29, 2009.
4. World Health Organization. Pandemic (H1N1) 2009-update 58. www.who.int/csr/don/2009-07-06/en/index.html. Accessed September 29, 2009.
5. Garcia-Garcia J, Ramos C. Influenza, an existing public health problem. Salud Publica Mex 2006; 48:244–267.
6. Perez-Padilla R, de la Rosa-Zamboni D, Ponce de Leon S, et al. Pneumonia and respiratory failure from swine-origin influenza A (H1N1) in Mexico. N Engl J Med 2009; 361:680–689.
7. Dawood FS, Jain S, Finelli L, et al. Emergence of a novel swine-origin influenza a (H1N1) virus in humans. N Engl J Med 2009; 360:2605–2615.
8. Agarwal P, Cinti S, Kazerooni E. Chest radiographic and CT findings in novel swine-origin influenza A (H1N1) virus (S-OIV) infection. AJR 2009; 193:1–6.
9. Lee C, Seo J, Song J, et al. Pulmonary complication of novel influenza A (H1N1) infection: imaging features in two patients. Korean J Radiol 2009; 10:531–534.
10. Marchiori E, Zanetti G, Hochhegger B, et al. High-resolution computed tomography findings from adult patients with Influenza A (H1N1) virus-associated pneumonia. Eur J Radiol. 2009 Dec 3. (Epub ahead of print).
11. World Health Organization. Clinical management of human infection with pandemic (H1N1) 2009: revised guidance. November 2009.
12. Fiore AE, Shay DK, Broder K, et al. Prevention and control of influenza: recommodations of the Advisory Committee on Immunization Practices (AFIP), 2008. MMWR Recomm Rep 2008; 57:1–60.
13. Kim EA, Lee KS, Primack SL, et al. Viral pneumonias in adults: radiologic and pathologic findings. Radiographics 2002; 22:S137–S149.